

**Supplementary data for
Molecular engineering of a high quantum yield NIR-II
molecular fluorophore with aggregation-induced emission
(AIE) characteristics for in vivo imaging**

Pengfei Xu^{#a,b}, Fei Kang^{#a}, Weidong Yang^{#a}, Mingru Zhang^a, Ruili Dang^b, Pei Jiang^{b*}
and Jing Wang^{a*}

^aDepartment of Nuclear Medicine, Xijing Hospital, Fourth Military Medical University. 710032. #127 West Changle Road, Xi'an, Shaanxi, China;

^bInstitute of Clinical Pharmacy & Pharmacology, Jining First People's Hospital, Jining Medical University, Jining 272000, P.R. China.

* Author of correspondence:

Dr. Pei Jiang, Institute of Clinical Pharmacy & Pharmacology, Jining First People's Hospital, Jining Medical University, Jining 272000, P.R. China. Email: jiangpeicsu@sina.com.

Prof. Jing Wang, Department of Nuclear Medicine, Xijing Hospital, Fourth Military Medical University. 710032. #127 West Changle Road, Xi'an, Shaanxi, China. Email: wangjing@fmmu.edu.cn

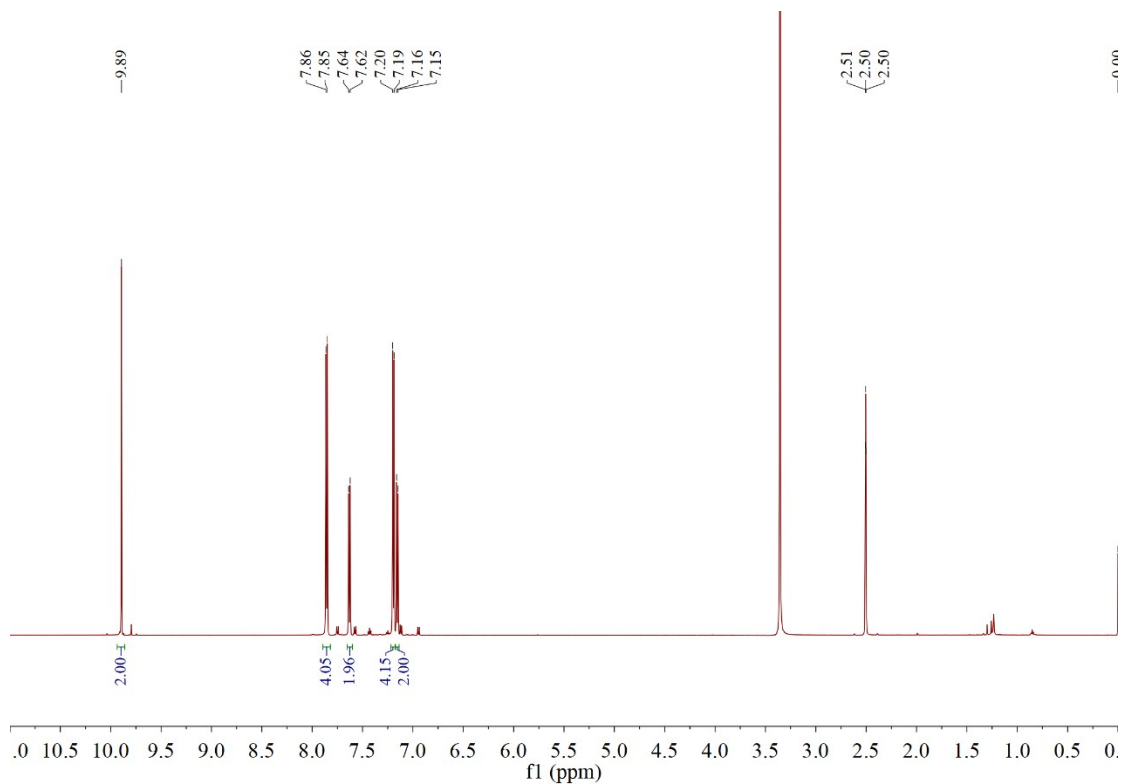


Figure S1. ^1H NMR spectrum of 4,4'-(4-bromophenyl)azanediyl)dibenzaldehyde in CDCl_3 .

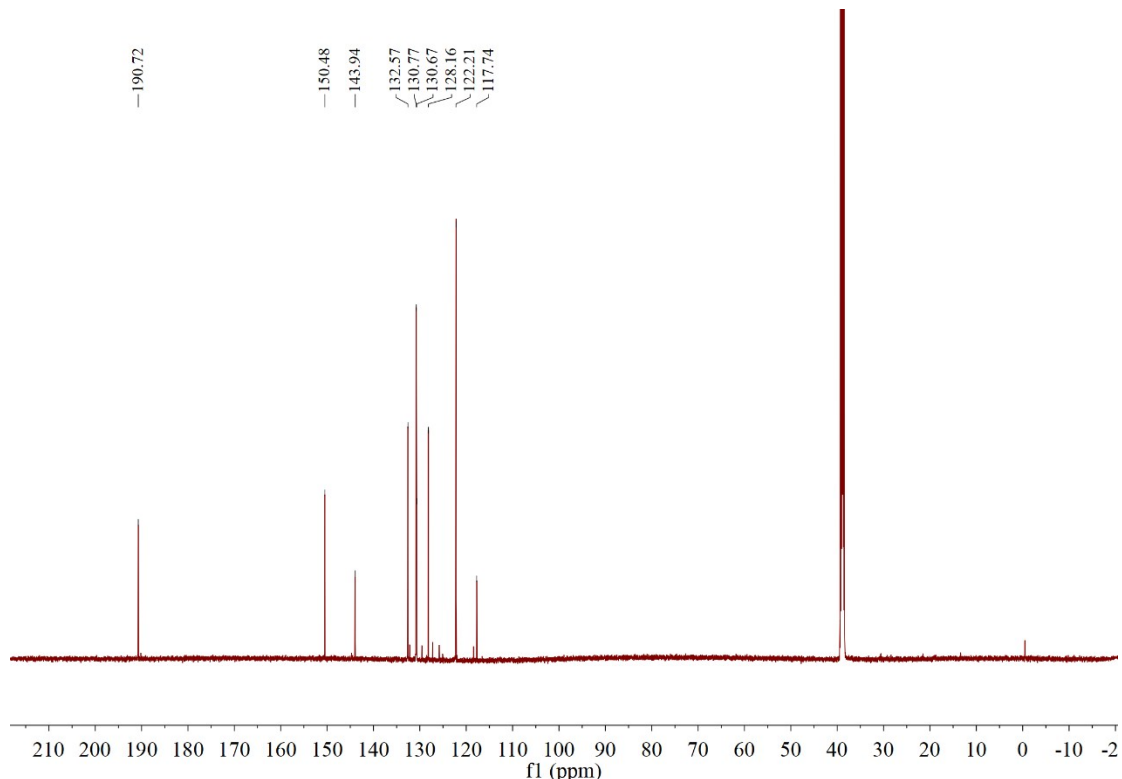


Figure S2. ^{13}C NMR spectrum of 4,4'-(4-bromophenyl)azanediyl)dibenzaldehyde in CDCl_3 .

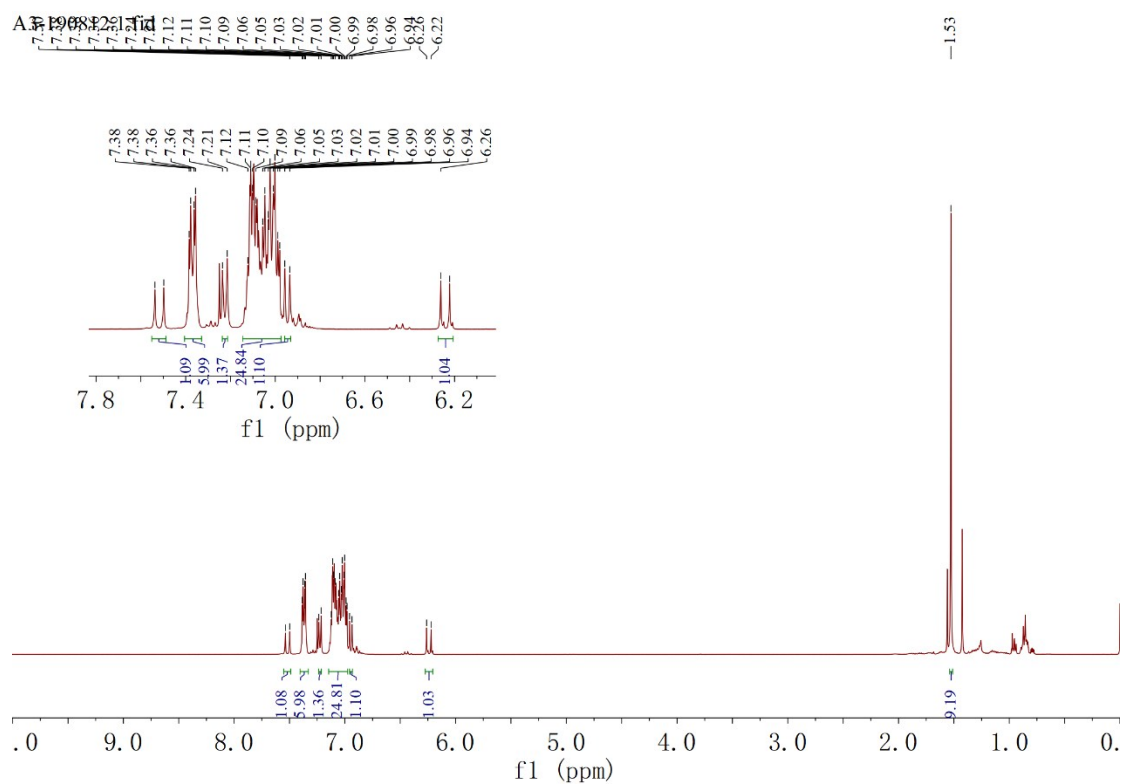


Figure S3. ^1H NMR spectrum of compound **3** in CDCl_3 .

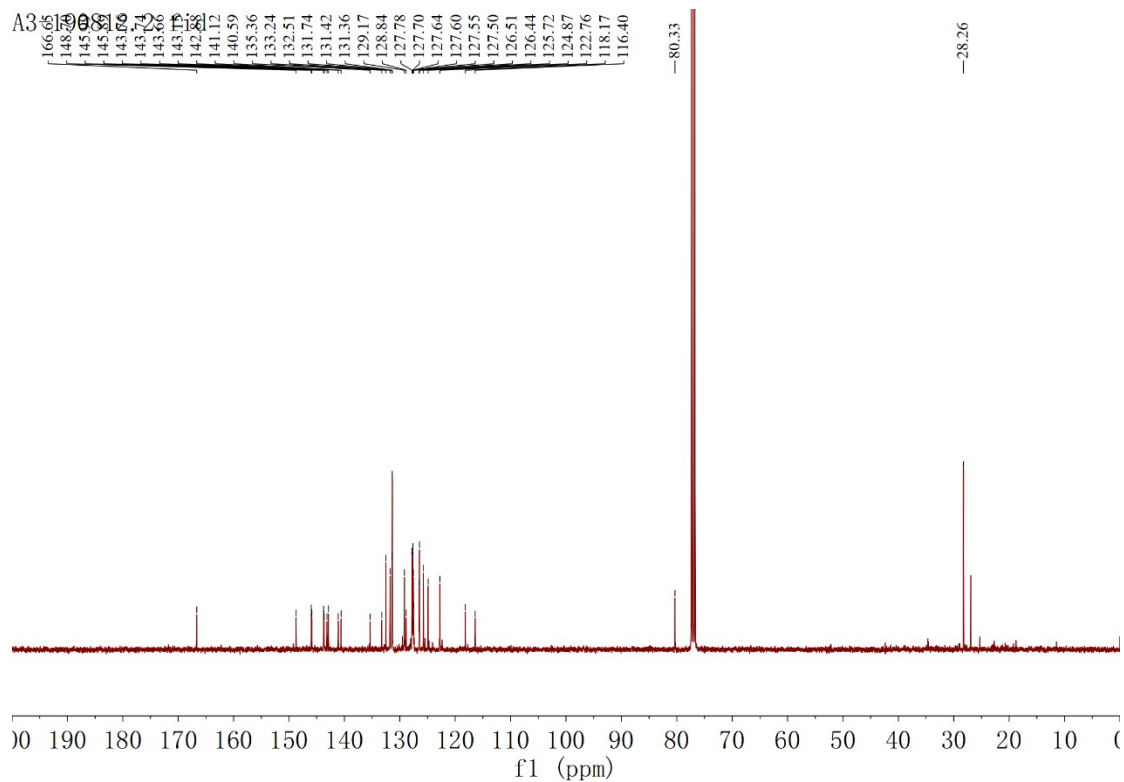


Figure S4. ^{13}C NMR spectrum of compound **3** in CDCl_3 .

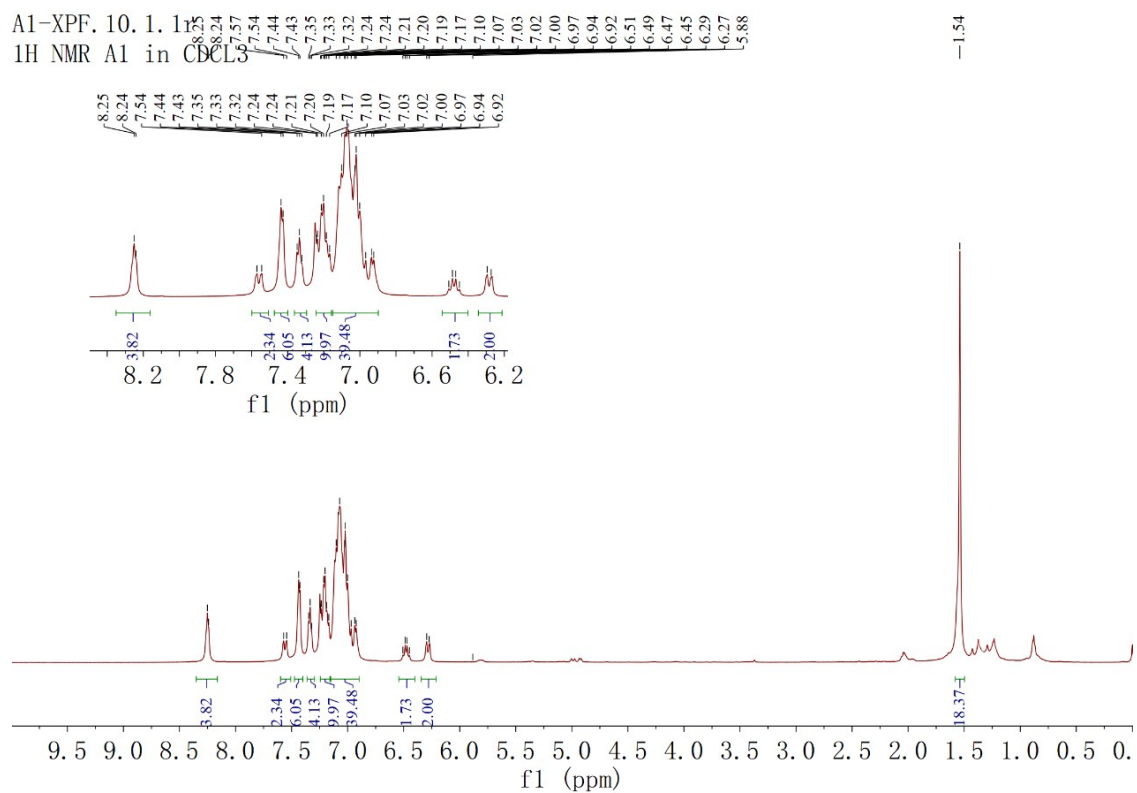


Figure S5. ^1H NMR spectrum of **XA1** in CDCl_3 .

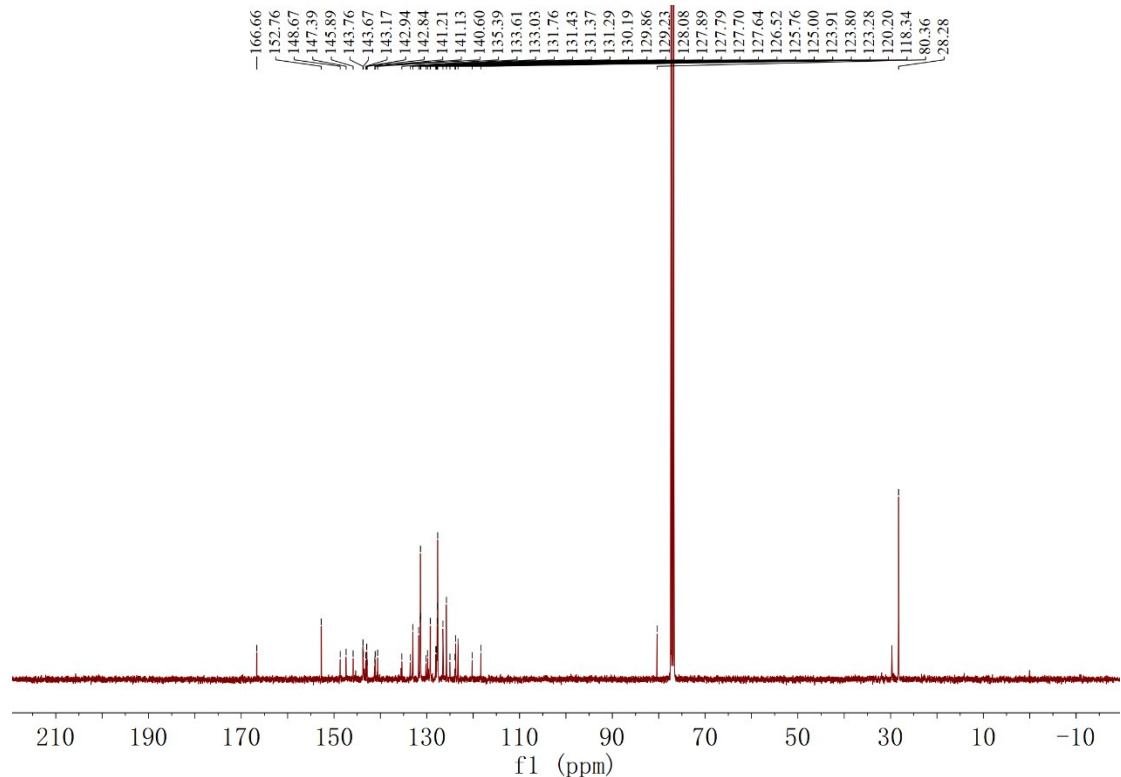


Figure S6. ^{13}C NMR spectrum of **XA1** in CDCl_3 .

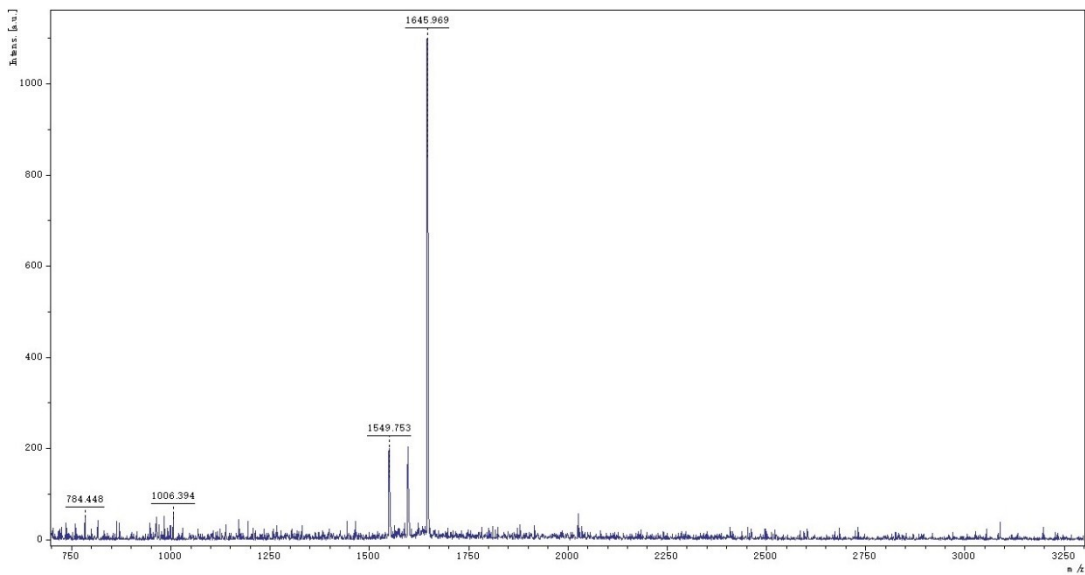


Figure S7. MALDI-TOF-MS measurement of **XA1**.

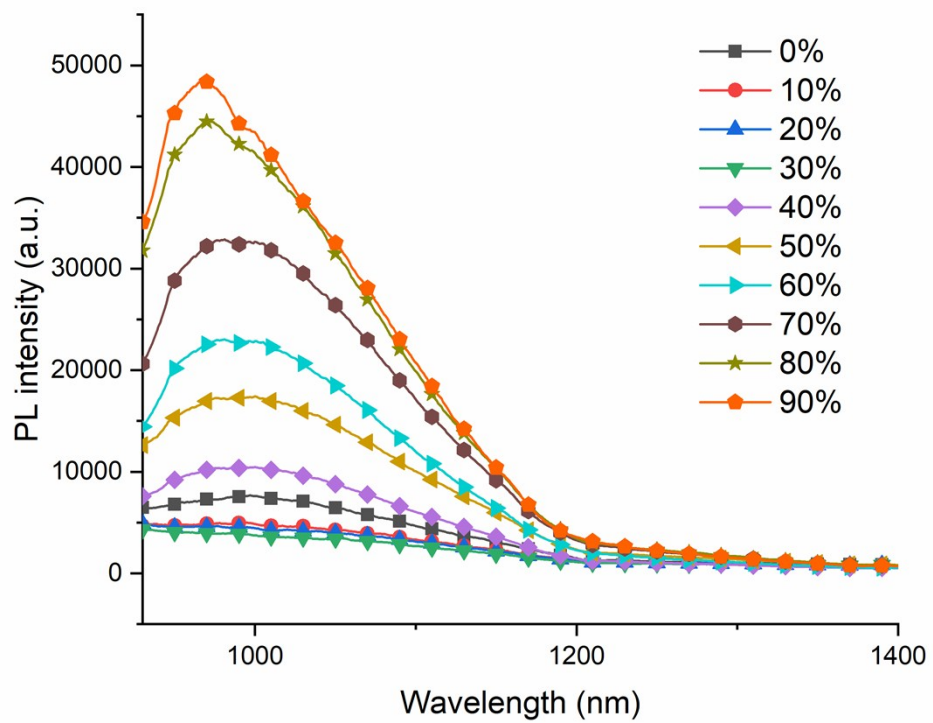


Figure S8. The emission spectra of **XA1** with different f_w .

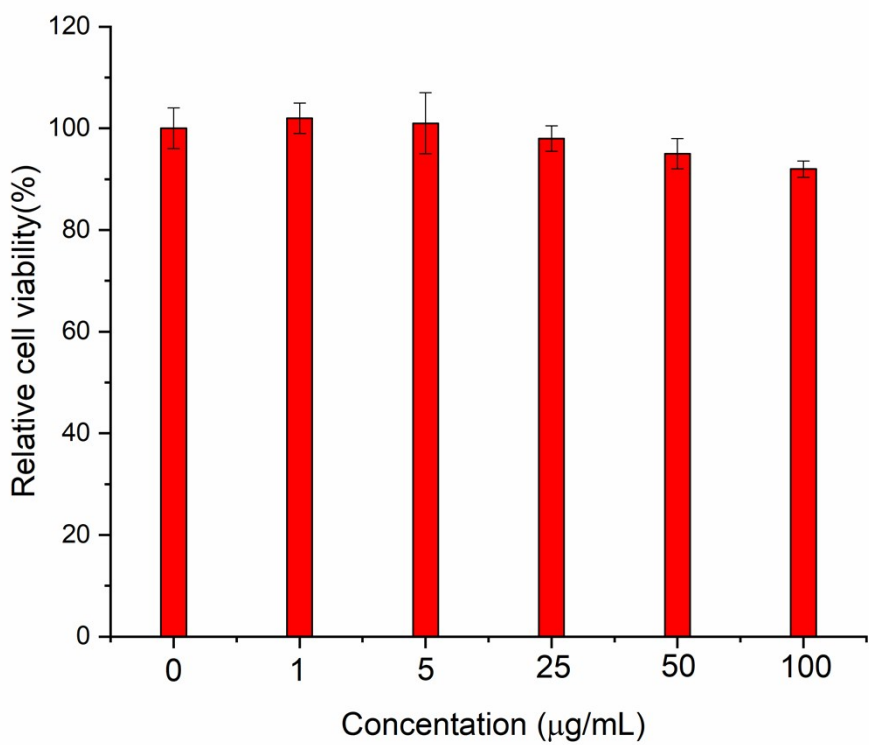


Figure S9. Cell viability of HeLa cells after incubation with aqueous dispersion of **XA1** NPs with various concentrations for 48 h.

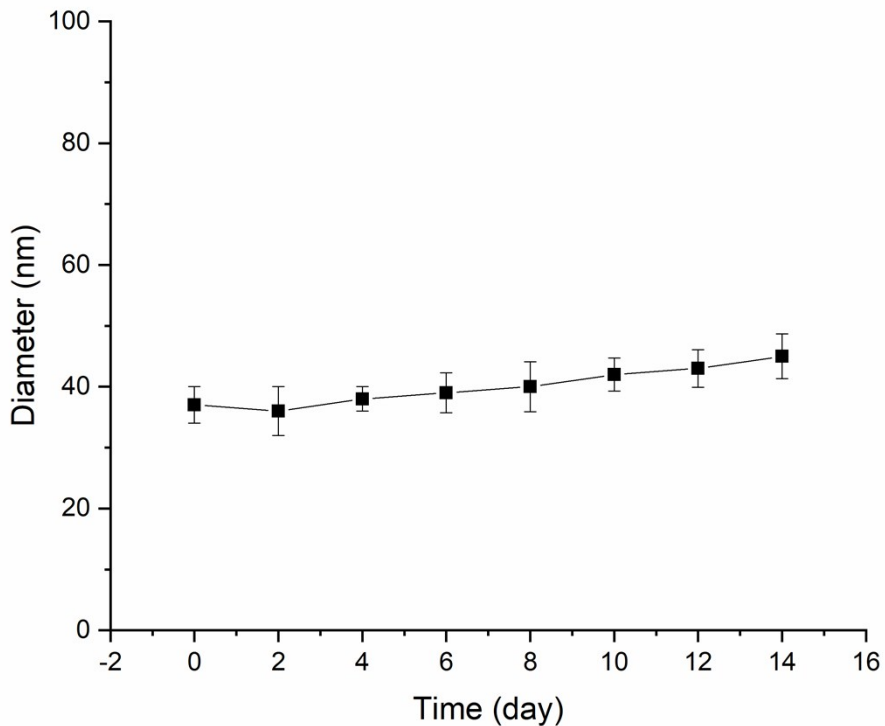


Figure S10. DLS results of XA1 NPs in water over 14 days.

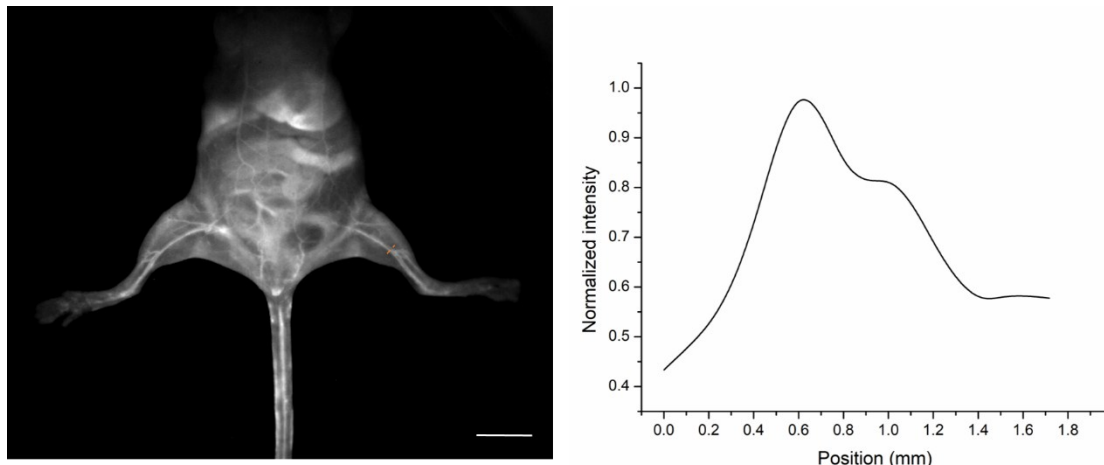


Figure S11. The line profile of the fluorescence intensity. Scale bar: 1 cm.

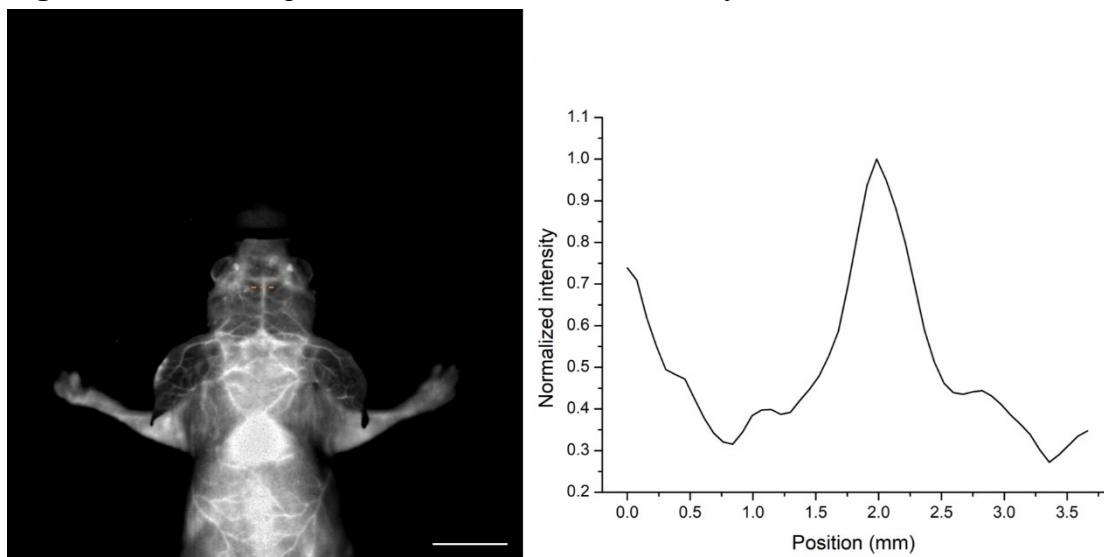


Figure S12. The line profile of the fluorescence intensity. Scale bar: 1 cm.

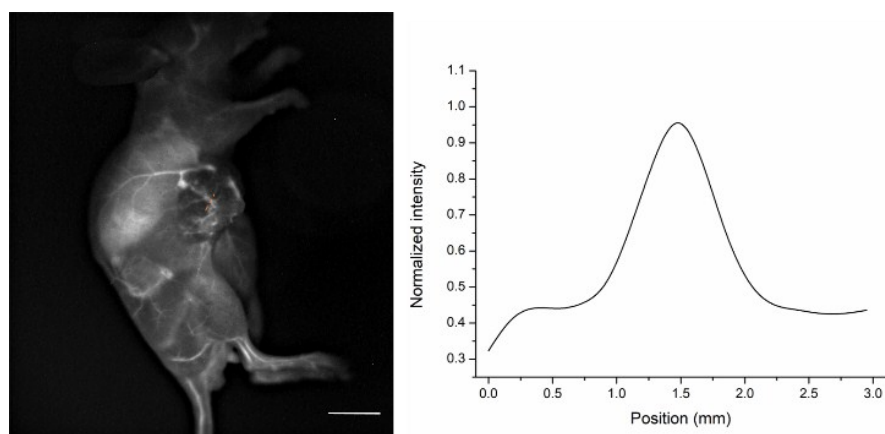


Figure S13. The line profile of the fluorescence intensity in the NIR II image of CT-

26 tumor-bearing nude mice (tumor size $\approx 0.75 \text{ cm}^3$). The image was captured at 1 min time points after a tail vein injection of **XA1** NPS. S/B=2.7 \pm 0.2.

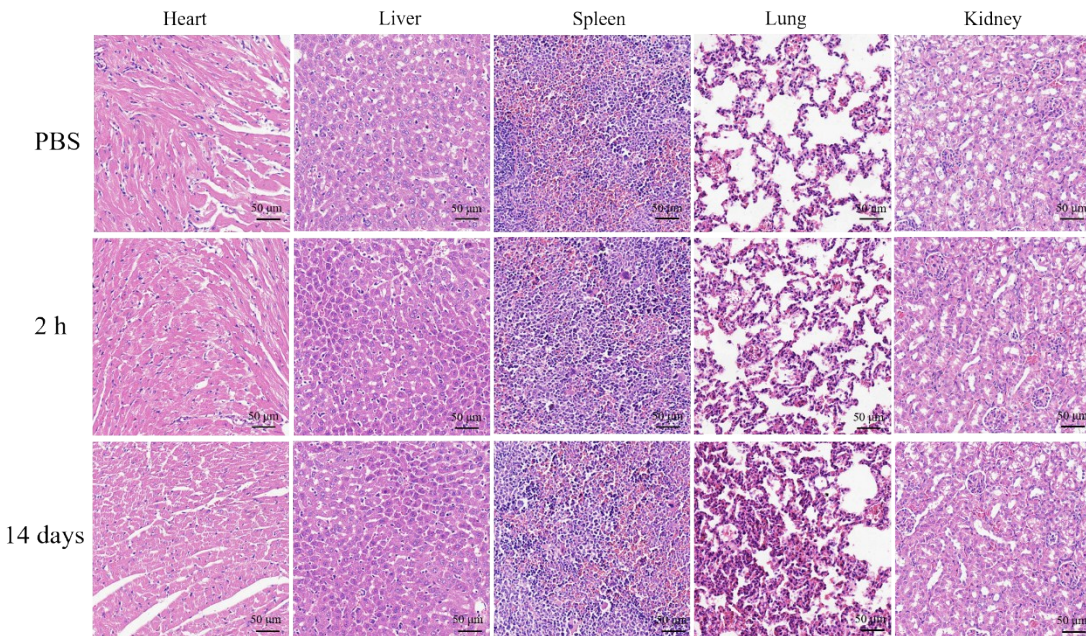


Figure S14. Histological H&E staining for main organs (heart, liver, spleen, lung and kidney) of the mice intravenously administrated with PBS and **XA1** NPs (10 times than the imaging doses, 5 mg of **XA1** per kg mouse) for 2 h and 14 days.

The QY of **XA1** was calculated according the previous reported calculation method.¹⁻³

$$\text{QY}_{\text{sample}} = \text{QY}_{\text{ref}} \frac{\text{slope}_{\text{sample}}}{\text{slope}_{\text{ref}}} \left(\frac{n_{\text{sample}}}{n_{\text{ref}}} \right)^2$$

The QYs were measured by the linear-regression plot of integrated fluorescent intensities at different concentrations on a molar basis. Where QY_{ref} of IR-26 in dichloroethane is 0.5%, and n_{sample} and n_{ref} are the refractive index of water and dichloroethane, respectively.

$$\text{QY} = 0.5\% \times \frac{29179925.14}{835364.08} \times \left(\frac{1.33}{1.4448} \right)^2 = 14.8\%$$

1. K. Cheng, H. Chen, C. H. Jenkins, G. Zhang, W. Zhao, Z. Zhang, F. Han, J. Fung, M. Yang, Y. Jiang, L. Xing and Z. Cheng, *ACS Nano*, 2017, **11**, 12276-12291.

2. Z. Sheng, B. Guo, D. Hu, S. Xu, W. Wu, W. H. Liew, K. Yao, J. Jiang, C. Liu, H. Zheng and B. Liu, *Adv Mater*,

2018, **29**, 1800766-1800774.

3. H. Wan, J. Yue, S. Zhu, T. Uno, X. Zhang, Q. Yang, K. Yu, G. Hong, J. Wang, L. Li, Z. Ma, H. Gao, Y. Zhong, J. Su, A. L. Antaris, Y. Xia, J. Luo, Y. Liang and H. Dai, *Nat Commun*, 2018, **9**, 1171.